
Successive Pruning for Model Compression via Rate Distortion Theory

Berivan Isik¹ Albert No² Tsachy Weissman¹

Abstract

Neural network (NN) compression has become essential to enable deploying over-parameterized NN models on resource-constrained devices. As a simple and easy-to-implement method, pruning is one of the most established NN compression techniques. Although it is a mature method with more than 30 years of history, there is still a lack of good understanding and systematic analysis of why pruning works well even with aggressive compression ratios. In this work, we answer this question by studying NN compression from an information-theoretic approach and show that rate distortion theory suggests pruning to achieve the theoretical limits of NN compression. Our derivation also provides an end-to-end compression pipeline involving a novel pruning strategy. That is, in addition to pruning the model, we also find a minimum-length binary representation of it via entropy coding. Our method consistently outperforms the existing pruning strategies and reduces the pruned model’s size by 2.5 times. We evaluate the efficacy of our strategy on MNIST, CIFAR-10 and ImageNet datasets using 5 distinct architectures.

1. Introduction

The recent success of NNs in various machine learning applications has come with their over-parameterization (Dean et al., 2012; LeCun et al., 2015). Deployment of such over-parameterized models on edge devices is challenging as these devices have limited storage, computation and power resources. Motivated by this, there has been significant interest in NN compression by the research community (Bucilua et al., 2006; Cheng et al., 2018).

Among various NN compression methods, pruning is a popular strategy with its intuitive foundation. It simply suggests

sparsifying a model by removing the “unimportant” weights to represent the model with fewer parameters and speed up the computations. Prior work differs in defining “importance” and they use different criteria to determine which weights to be pruned (Williams, 1995; Castellano et al., 1997; Engelbrecht, 2001; Srinivas & Babu, 2015; Molchanov et al., 2016; 2017; He et al., 2017; Lin et al., 2017a; Anwar et al., 2017; Yang et al., 2017; Carreira-Perpinán & Idelbayev, 2018; Yu et al., 2018; Liu et al., 2018a;b; 2019; Lin et al., 2019; Xiao et al., 2019; Gale et al., 2019; Zhao et al., 2019; Peng et al., 2019; Frankle et al., 2020; Sehwag et al., 2020; Blalock et al., 2020; Wang et al., 2020b). For instance, (Han et al., 2015; 2016; Frankle & Carbin, 2019) prune the weights with small magnitudes, (Cun et al., 1990; Hassibi et al., 1993; Singh & Alistarh, 2020) prune the weights which contribute less to the Hessian matrix of the loss function and (Lee et al., 2018) prune the weights with small connection sensitivity. Although each strategy follows a different path, they all achieve compressing the model aggressively (up to 90% pruning for moderate size NN models) without considerable performance degradation. However, they do not provide a theoretical background as to why pruning works so well in the first place. Currently, there is a lack of satisfying explanation and systematic analysis of why removing a significant fraction of the parameters from the model does not harm the NN performance. In this work, we find an answer to this question by studying NN compression from an information-theoretic approach and prove, via rate distortion theory, that the optimal method that achieves the theoretical limits of NN compression is pruning.

Rate distortion theory provides the fundamental trade-off between the rate (number of bits per weight) and the distortion (the difference between the original and the reconstructed models). More precisely, if the distribution of the weights and the distortion metric are given, we can compute the exact rate distortion trade-off and construct the optimal compression scheme. While prior work assumes Gaussian distribution over NN weights (Gao et al., 2019), we demonstrate with 5 architectures on 3 datasets that Laplace distribution is a better fit than Gaussian. Following the observation of (Isik et al., 2021) that the sign of the weights plays a critical role in the NN performance, we store the sign information separately and compress only the sign-free weights. This

¹Department of Electrical Engineering, Stanford University, Stanford, US ²Department of Electronic and Electrical Engineering, Hongik University, Seoul, South Korea. Correspondence to: Berivan Isik <berivan.isik@stanford.edu>.

leaves an exponential distribution over the magnitude of NN weights. An interesting property of the optimal compression scheme for exponential source is the sparsity of the reconstruction, i.e., most of the weights in the reconstructed model are 0. This naturally suggests pruning.

Our findings from rate distortion theory also introduce a novel pruning strategy that is fundamentally different from the previous work. In order to encode the pruned model as a binary sequence, we first need an efficient discrete representation of the model. Existing pruning methods outputs a sparse model, which can be represented as a list of tuples (i, w_i) where i and w_i are the location and value of a particular nonzero weight after pruning. Since it is hard to characterize the distribution of i and w_i , the entropy coding for these tuples may not be optimal. On the other hand, we show that our pruning strategy directly outputs a list of integers that follow a geometric distribution and these integers reconstruct the pruned model. The fact that these integers have a well-known distribution allows us to apply a simple optimal entropy coding method to encode them. Thus, different from the previous work, our strategy provides an end-to-end compression of a NN model, which involves both pruning and entropy coding. We call our strategy “successive pruning” as our rate distortion theoretic optimal compression scheme is based on successive refinement (Koshelev, 1980; Equitz & Cover, 1991), meaning that we describe the weights iteratively and at each iteration, the reconstructed model becomes closer to the original model.

Lastly, we demonstrate that our assumption of Laplace distribution over NN weights holds for NN gradients as well. Therefore, our strategy provides a tool for compressing NN gradients, an important objective in communication-efficient federated learning settings (Kairouz et al., 2019).

The contributions of our paper can be summarized as:

1. We prove that pruning is the rate distortion theoretic optimal NN compression method.
2. We introduce a novel end-to-end NN compression technique that, different from the prior work, jointly prunes the model and finds its minimum-length binary representation.
3. We show that these methods are applicable for communication-efficient federated learning as well.

We demonstrate the efficacy of our strategy through extensive experiments on MNIST, CIFAR-10 and ImageNet datasets with 5 distinct architectures. We compare our method with existing pruning strategies and show that successive pruning outperforms the others in all settings with up to 2.5 times more efficient binary representation for the pruned model.

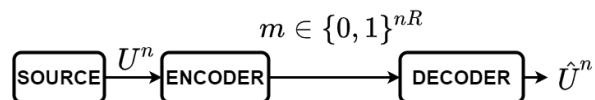
2. Preliminaries

In this section, we present the problem setup, briefly introduce the rate distortion theory and successive refinement, and empirically show that NN weights can be modelled by a Laplace distribution.

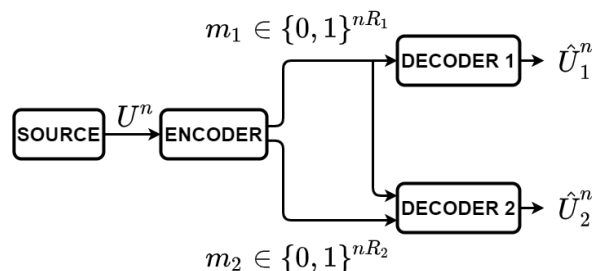
2.1. Problem Statement and Notation

We study a supervised learning problem where NN parameters w are trained to learn a conditional distribution $p_w(y|x)$ of labels y given the inputs x . During the training, the model has access to samples $\mathcal{D} = \{(x_i, y_i)\}_{i=1}^m$ drawn from the data distribution $(x, y) \sim p_{x,y}$. The performance metric in our learning problem is the accuracy of the prediction $p_w(y|x)$ on the test data drawn from the same distribution $p_{x,y}$. We aim to compress w to represent the model with the minimum number of bits while preserving the accuracy of the model. This is a lossy compression problem where the distortion is a measure of the distance between the original model and compressed model, and the rate is the number of bits required to represent one weight. In information-theoretic term, rate distortion theory characterizes the minimum achievable rate given the target distortion.

More precisely, let $\mathbf{U}_1, \dots, \mathbf{U}_n \in \mathcal{U}$ be a source sequence generated by i.i.d. $\sim p(u)$. The encoder $f_e : \mathcal{U}^n \rightarrow \{0, 1\}^{nR}$ describes this sequence in nR bits, where this binary representation is called a “message” m . The decoder $f_d : \{0, 1\}^{nR} \rightarrow \hat{\mathcal{U}}^n$ reconstructs an estimate $\hat{u}^n \in \hat{\mathcal{U}}^n$ based on $m \in \{0, 1\}^{nR}$. This process, summarized in Figure 1(a), is called source coding.



(a) Source Coding.



(b) Successive Refinement.

Figure 1. (a) Source Coding, (b) Successive Refinement with 2 Decoders.

The number of bits per source symbol ($\frac{nR}{n} = R$ in this case) and the “distance” $D(u^n, \hat{u}^n) = \sum_{(u, \hat{u})} d(u, \hat{u})$ between

u^n and \hat{u}^n are named as rate and distortion, respectively. Ideally, we would like to keep both rate and distortion low, but there is a trade-off between these two quantities, which is characterized by the rate-distortion function (Shannon, 2001; Berger, 2003; Cover & Thomas, 2006) as:

$$R(D) = \min_{p(\hat{u}|u): \sum_{(u, \hat{u})} p(u)p(\hat{u}|u)d(u, \hat{u}) \leq D} I(\mathbf{U}; \hat{\mathbf{U}}) \quad (1)$$

where $I(\mathbf{U}; \hat{\mathbf{U}})$ is the mutual information between \mathbf{U} and $\hat{\mathbf{U}}$, and $d(u, \hat{u})$ is a predefined distortion metric, e.g. ℓ_2 distance. The rate-distortion function $R(D)$ in Eq. 1 is the minimum achievable rate at distortion D , and the conditional distribution $p(\hat{u}|u)$ that achieves $I(\mathbf{U}; \hat{\mathbf{U}}) = R(D)$ explains how an optimal encoder-decoder pair should operate for the source $p(u)$. Clearly, source distribution has a critical role in the solution of the rate distortion problem. We discuss possible assumptions for the distribution of NN weights in the next section.

Throughout the paper, $w \in \mathbb{R}^n$ is the weights of a trained model, $f_L(u; \mu, b) = \frac{1}{2b} \exp\left(-\frac{|u-\mu|}{b}\right)$ is the probability density function (pdf) of Laplace distribution with mean μ and scale b , $f_{\text{exp}}(u; \lambda) = \lambda e^{-\lambda u}$ is the pdf of exponential distribution with parameter λ . Logarithms are in base 2 and rate is defined as bits per symbol. We define the compression rate as the ratio of the original model size to the compressed model's size, where size is the length of the model's binary representation.

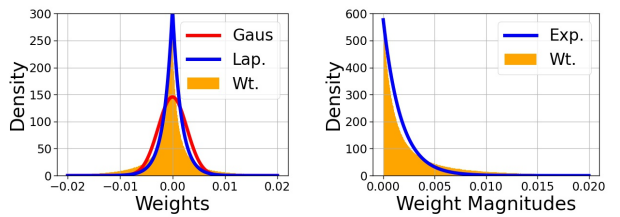
2.2. Density of Neural Network Parameters

In order to apply the rate distortion theory for NN compression, we need a good density estimation for the NN weights. Figure 2(a) shows the density of ResNet-18 weights trained on CIFAR-10, and corresponding Gaussian and Laplacian distributions having the same mean and variance. While prior work assumes Gaussian distribution for the underlying distribution of NN weights (Gao et al., 2019), Figure 2(a) suggests that zero-mean Laplacian distribution is a better fit. Apart from being a better approximation to the distribution of NN weights, Laplacian distribution has another appealing property:

$$u \sim f_L(u; \mu, b) \Rightarrow |u - \mu| \sim f_{\text{exp}}\left(u; \frac{1}{b}\right).$$

That is, if u is a sample from a Laplacian source with mean μ and scale b , then $|u - \mu|$ has an exponential distribution with parameter $\frac{1}{b}$. Figure 2(b) shows that exponential distribution almost perfectly matches the magnitude of NN weights. This observation enables us to study the compression of sign-free weights by applying rate distortion theory to the exponential source. The reason why we discard sign bits follows the conclusion of (Isik et al., 2021). They show that small perturbations on the weights may lead to sign errors that degrade the NN performance significantly. Thus, we

keep the sign bits as they are and compress the sign-free weights. We refer the reader to Appendix A for density plots of ResNet-50, VGG-16, LeNet-5-Caffe, and LeNet-300-100.



(a) Density of Weights. (b) Density of Sign-Free Weights.

Figure 2. Density of ResNet-18 (a) Signed Weights, (b) Sign-free Weights. ResNet-18 is trained on CIFAR-10. Gaus: Gaussian, Lap.: Laplacian, Exp.: Exponential, Wt.: NN Weights.

2.3. Successive Refinement

In the successive refinement problem, summarized in Figure 1(b), the encoder wants to describe the source to two decoders, where each decoder has its own target distortion, D_1 and D_2 . Instead of having separate encoding schemes for each decoder, the successive refinement encoder encodes a message m_1 for Decoder 1 (with higher target distortion, D_1), and encodes an extra message m_2 where the second decoder gets both m_1 and m_2 . Receiving both m_1 and m_2 , Decoder 2 reconstructs $\hat{\mathbf{U}}_2^n$ with distortion D_2 . Since the message m_1 is re-used, the performance of successive refinement encoder is sub-optimal in general. However, in some cases, the successive refinement encoder achieves the optimum rate distortion trade-off as if dedicated encoders were used separately. In such a case, we call the source (distribution) and the distortion pair “successively refinable” (Koshelev, 1980; Equitz & Cover, 1991).

The idea of successive refinement can be utilized to reduce the complexity of the information-theoretic optimal compression scheme. The optimum scheme in rate distortion theory finds the message m that codes the best reconstruction $\hat{\mathbf{U}}$ from the codebook of size 2^{nR} (see Figure 1(a)). This is not implementable in practice due to the exponential complexity. The successive refinement encoder in Figure 1(b) can find the best reconstruction iteratively, and therefore can reduce the complexity. Instead of searching over 2^{nR} codewords, the successive refinement encoder finds m_1 that codes a sub-codeword from the sub-codebook of size 2^{nR_1} , and m_2 that codes a sub-codeword from another sub-codebook of size 2^{nR_2} where $R_1, R_2 \approx R/2$. Then, the complexity in successive refinement, $2^{nR_1} + 2^{nR_2}$, is smaller than that of one-step source coding, 2^{nR} . We can increase the number of steps (number of decoders) to reduce the complexity fur-

ther. For Gaussian source under mean squared error, which is also successively refinable, (Venkataramanan et al., 2014) and (No & Weissman, 2016) generalize the idea of successive refinement, and propose low complexity schemes that achieve the optimum rate distortion trade-off curve. Note that the exponential source under one-sided ℓ_1 loss is also successively refinable. In this paper, we propose a practical low complexity compression scheme for exponential source based on successive refinement, which also provides a novel pruning strategy for NN compression.

3. Methodology

In this section, we study lossy compression of exponential sources (Section 3.1), and present ways to apply our findings in NN compression (Section 3.2) and communication-efficient federated learning (Section 3.3) problems.

3.1. Compression for Exponential Source

3.1.1. LOSSY COMPRESSION

We consider i.i.d. exponential source sequence u_1, \dots, u_n with distribution $f_{exp}(u; \lambda) = \lambda e^{-\lambda u}$ for $u \geq 0$, reconstruction v_1, \dots, v_n , and one-sided ℓ_1 distortion given by:

$$d(u, v) = \begin{cases} u - v, & \text{if } u \geq v \\ \infty, & \text{otherwise.} \end{cases}$$

We start with the rate distortion function which is a minimum achievable rate given the target distortion D :

Lemma 1. (Verdu, 1996) *The rate distortion function for an exponential source with one-sided distortion is given by*

$$R(D) = \begin{cases} -\log(\lambda D), & 0 \leq D \leq \frac{1}{\lambda} \\ 0, & D > \frac{1}{\lambda} \end{cases} \quad (2)$$

with the following optimal conditional probability distribution that achieves the minimum mutual information

$$f_{\mathbf{U}|\mathbf{V}}(u|v) = \begin{cases} \frac{1}{D} e^{-(u-v)/D}, & u \geq v \geq 0 \\ 0, & \text{otherwise.} \end{cases} \quad (3)$$

Moreover, the marginal distribution of \mathbf{V} is as follows

$$f_{\mathbf{V}}(v) = \lambda D \cdot \delta(v) + (1 - \lambda D) \cdot \lambda e^{-\lambda v} \quad (4)$$

where $\delta(v)$ is a Dirac measure at 0. The proofs of Lemma 1 and Eq. 4 are given in Appendix B.1. The sparsity of \mathbf{V} in Eq. 4 suggests pruning as an optimal compression strategy!

Note that the distribution of $\mathbf{U} - \mathbf{V}$ given $\mathbf{V} = v$ is exponential with parameter $1/D$. Based on this property, we can design an explicit successive refinement encoder. Instead

of a successive refinement scheme with two decoders as described in Section 2.3, we consider the successive refinement problem with L decoders. Let $\lambda = \lambda_0 < \lambda_1 < \dots < \lambda_L$ where $D_t = 1/\lambda_t$ is a target distortion at the t -th decoder. We begin by setting $\mathbf{U}^{(0)} = u^n$. At t -th iteration, the encoder finds $\mathbf{V}^{(t)}$ that minimizes the distance between $D(\mathbf{U}^{(t-1)}, \mathbf{V}^{(t)})$ from the codebook $\mathcal{C}^{(t)}$, then computes $\mathbf{U}^{(t)} = \mathbf{U}^{(t-1)} - \mathbf{V}^{(t)}$. The t -th codebook consists of codewords generated by the marginal distribution in Eq. 4:

$$f_{\mathbf{V}^{(t)}}(v) = \frac{\lambda_{t-1}}{\lambda_t} \cdot \delta(v) + \left(1 - \frac{\lambda_{t-1}}{\lambda_t}\right) \cdot \lambda_{t-1} e^{-\lambda_{t-1} v}$$

Since $\mathbf{U}^{(t)}$ is an i.i.d. exponential random sequence from Eq. 3, the encoder can keep applying the compression schemes for exponential sources at each iteration. At iteration t , the reconstruction on the decoder side is $\hat{\mathbf{U}}^{(t)} = \sum_{\tau=1}^t \mathbf{V}^{(\tau)}$. In summary, for $1 \leq t \leq L$, the original information-theoretic successive refinement encoder performs the following steps iteratively:

1. Find $\mathbf{V}^{(t)} \in \mathcal{C}^{(t)}$ that minimizes $D(\mathbf{U}^{(t-1)}, \mathbf{V}^{(t)})$.
2. Update \mathbf{U} as $\mathbf{U}^{(t)} = \mathbf{U}^{(t-1)} - \mathbf{V}^{(t)}$.

We further simplify the above algorithm by a heuristic approach which does not require to generate random codewords or compute the distortion between $\mathbf{U}^{(t-1)}$ and $\mathbf{V}^{(t)}$ at each iteration. The heuristic coding scheme is as follows:

1. Find index i such that $\mathbf{U}_i^{(t-1)} \geq \frac{1}{\lambda_{t-1}}$. If there are more than one such indices, pick an index i randomly. Encode i as m_t .
2. Let $\mathbf{V}^{(t)}$ be an n -dimensional all-zero vector except $\mathbf{V}_i^{(t)} = \frac{1}{\lambda_{t-1}}$.
3. Let $\mathbf{U}^{(t)} = \mathbf{U}^{(t-1)} - \mathbf{V}^{(t)}$.
4. Set $\lambda_t = \frac{n}{n-1} \cdot \lambda_{t-1}$.

This coding scheme is equivalent to the original scheme, where $\frac{\lambda_{t-1}}{\lambda_t} = \frac{n-1}{n}$ for $1 \leq t \leq L$, and the codebook $\mathcal{C}^{(t)}$ consists of n -dimensional all-zero vectors except a single nonzero element of value $\frac{1}{\lambda_{t-1}}$. We call our scheme ‘‘successive pruning’’ as it can be used to prune NN weights (see Section 2.3). Algorithm 1 shows how to implement successive pruning to compress an exponential source sequence, e.g., NN weights, and Figure 3 illustrates how it outputs a sparse vector $\hat{\mathbf{U}}^{(3)}$ by reconstructing $\mathbf{U}^{(0)}$ iteratively. Notice that the encoder needs to send the decoder only an index $i \in \{1, \dots, n\}$ for each iteration. In other words, the encoder does not communicate any continuous variable except the mean of the initial exponential distribution. When there is no index i such that $\mathbf{U}_i^{(t-1)} \geq \frac{1}{\lambda_{t-1}}$,

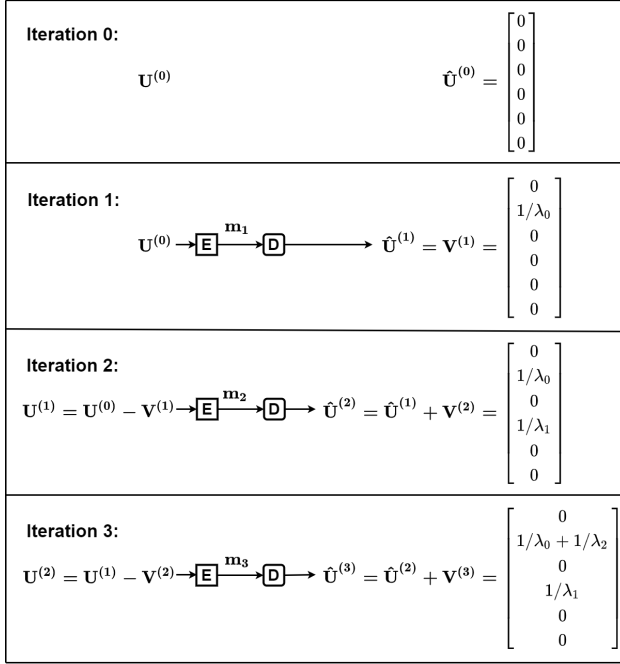


Figure 3. Successive Pruning. E: Encoder, D: Decoder.

the encoder re-estimates the empirical mean and sends a refreshed $1/\lambda$ to the decoder. However, this is a rare situation in our experiments (20 refreshments in 20M iterations) and hence has a negligible effect on the size of the compressed model.

3.1.2. LOSSLESS COMPRESSION (ENTROPY CODING)

Our coding scheme requires communicating an index $i \in \{1, \dots, n\}$ from the encoder to the decoder for each iteration. We need a lossless compression scheme, namely entropy coding, to represent these indices as binary sequences. In information theory, the optimal entropy coding method can be found when the source distribution is known in advance (Huffman, 1952). Although there are universal codes that encode any source regardless of the distribution, they are preferable only when the source distribution is unknown since an entropy coding that matches the source distribution is always better than a universal code. Fortunately, our coding scheme for exponential source induces a well-defined distribution that allows us to choose an optimal entropy coding method. Notice that randomly picking an index i from $\{j : \mathbf{U}_j^{(t)} \geq \frac{1}{\lambda_t}\}$ is equivalent to; (1) first randomly permuting $\mathbf{U}^{(t)}$, and (2) selecting the minimum index i from $\{j : \mathbf{U}_j^{(t)} \geq \frac{1}{\lambda_t}\}$. The second approach induces a geometric distribution under the i.i.d. assumption on the indices where small indices are always more probable to be selected. For geometric sources, there are two standard entropy coding methods: unary coding and Golomb coding (Golomb, 1966; Gallager & Van Voorhis, 1975). Details about these entropy

Algorithm 1 Successive Pruning

Hyperparameters: scale factor α for empirical mean

Inputs: exponential sequence u_1, \dots, u_n with n symbols

Output: reconstructed sequence $u_1^{recon}, \dots, u_n^{recon}$

$(u_1^{recon}, \dots, u_n^{recon}) \leftarrow 0$

$\lambda \leftarrow \text{MeanEst}((u_1, \dots, u_n))$

Encoder sends λ to the Decoder.

for $t = 1, \dots, L$ **do**

Encoder:

$m_{inds} \leftarrow$ (indices of the components in (u_1, \dots, u_n) that are larger than $1/\lambda$.)

if m_{inds} is empty **then**

$\lambda \leftarrow \text{MeanEst}((u_1, \dots, u_n))$

sends λ to the Decoder.

end if

$m \leftarrow$ (a random index from m_{inds})

sends m to the Decoder.

$u_m = u_m - 1/\lambda$

$\lambda \leftarrow \frac{n}{n-1} \cdot \lambda$

Decoder:

receives m from the Encoder.

$u_m^{recon} = u_m^{recon} + 1/\lambda$

$\lambda \leftarrow \frac{n}{n-1} \cdot \lambda$

end for

MeanEst $((u_1, \dots, u_n))$:

$1/\lambda \leftarrow$ mean of (u_1, \dots, u_n)

$\lambda \leftarrow \alpha \cdot \lambda$

return λ

coding methods are given in Appendix B.2. Although both unary coding and Golomb coding show comparable rate distortion trade-off to the rate distortion function in Eq. 2, we use Golomb coding in our experiments.

3.2. Successive Pruning for Model Compression

Finally, we propose successive pruning, a NN compression strategy that combines the iterative coding scheme presented in Algorithm 1 with Golomb coding. Since exponential distribution matches well with the sign-free NN weights, we directly apply Algorithm 1 to the sign-free weights of a fully-trained NN. We show the accuracy and sparsity of the reconstructed ResNet-50 (on ImageNet) through iterations in Figure 4. Notice that the sparsity in the reconstructed weights is 100% at the first iteration, and it decreases as the decoder receives new indices from the encoder (as in Figure 3). As the iterations proceed, we are able to recover the accuracy of the original model (see Figure 4(b)).

Retraining the pruned model to tune the non-pruned weights is a widely accepted procedure, and it usually boasts the accuracy in higher compression ratios. We adopt this approach by running successive pruning in two phases, as shown in

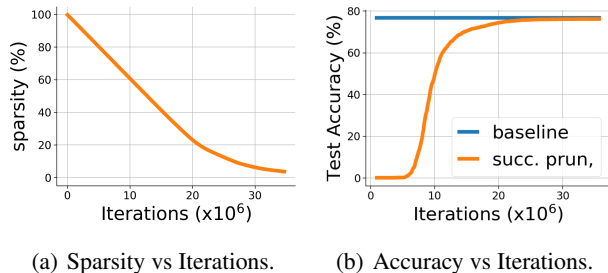


Figure 4. Sparsity and Accuracy of the Reconstructed ResNet-50 on ImageNet. succ. prun.: Successive Pruning.

Figure 5. In phase-1, we apply successive pruning to the non-pruned weights w until we reach a desired sparsity s (sparsity is always non-increasing, see Figure 4(a)). Once we get the sparsity s , we stop the successive pruning algorithm and construct a pruning mask $\mathcal{M}_p \in \{0, 1\}^n$ based on the nonzero elements’ locations in the reconstructed weight \hat{w} , i.e., if $\hat{w}_i > 0$, then $\mathcal{M}_{p,i} = 1$. We use \mathcal{M}_p to prune the original weights w , i.e., $w_{\text{pruned}} = \mathcal{M}_p \odot w$. From the weights w_{pruned} , we retrain the nonzero ones for a few epochs and call the retrained weights by $w_{\text{retrained}}$. After resetting the reconstructed weights $\hat{w} = 0$, we start phase-2. During phase-2, we apply successive pruning to $w_{\text{retrained}}$ which has sparsity s . At the end of phase-2, we have a reconstructed weight \hat{w} whose sparsity is lower bounded by s . In short, phase-1 outputs a pruning mask that is used to prune the model whereas phase-2 is devoted to finding the binary representation of the pruned and retrained model. With this 2-phase approach, successive pruning consistently outperforms existing pruning strategies in terms of accuracy-sparsity trade-off (output of retraining in Figure 5), and we achieve a comparable (mostly better) compression rates (output of phase-2 in Figure 5). Since we apply the successive pruning algorithm to a retrained pruned model in phase-2, we need an exponential distribution over weights of this model as well. We verify that exponential distribution is still a good fit for retrained model’s nonzero and sign-free weights through density plots in Appendix C.

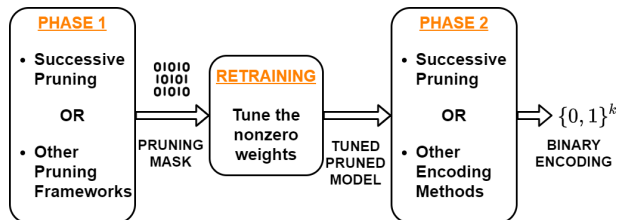


Figure 5. End-to-End NN Compression with Successive Pruning.

Successive pruning differs from the existing pruning and encoding methods in the way how the pruned model is encoded. (Han et al., 2016) propose iterative magnitude prun-

ing with retraining to find the pruning mask \mathcal{M}_p (phase-1 and retraining). After the pruned model $w_{\text{pruned}} = \mathcal{M}_p \odot w$ is constructed, they represent this model as a list of tuples (i, w_i) , where i and w_i are the location and value of a nonzero weight. They use compressed sparse row (CSR) or compressed sparse column (CSC) formats to efficiently code the relative indices $i - j$, where j is the index of the previous nonzero weight. They put a limit for the maximum allowable relative index to keep the bit representation shorter. If there are no nonzero weights in the range, the encoder puts a filler zero. Since each weight w_i is a 32-bit floating-point, they quantize w_i ’s to represent weights more efficiently. Lastly, they apply Huffman coding for both relative indices $i - j$ and weights w_i (Van Leeuwen, 1976). There are three main problems with this approach: (1) the trick with filler zeros to limit the number of bits per relative index is inefficient for high sparsity ratios, (2) quantization of the weights brings additional accuracy loss and requires extra tuning steps, and (3) the distribution used for Huffman coding needs to be encoded as well. (Wiedemann et al., 2020) do not propose a new pruning framework but show promising results with context-aware binary arithmetic coding (CABAC) in encoding a pruned model (Marpe & Wiegand, 2003). That is, they take a retrained pruned model and encode it via CABAC (phase-2). While both (Han et al., 2016) and (Wiedemann et al., 2020) encode a pruned model in a lossy way, our method directly applies Golomb coding to the output of successive pruning algorithm (geometrically distributed indices). In other words, our end-to-end compression method has three advantages over the existing approaches: (a) it does not require an additional lossy and costly step such as quantization before encoding, (b) it only encodes discrete-valued indices instead of floating points (e.g., weight values), and (c) the entropy coding method perfectly matches the predefined distribution of the indices, i.e., it is optimal.

We underline that successive pruning can be combined with other pruning or encoding strategies. As shown in Figure 5, we can use any pruning strategy in phase-1 and encode the pruned model with successive pruning in phase-2, or we can use successive pruning in phase-1 as a pruning framework and encode the pruned model with other methods such as CSR+quantization+Huffman and CABAC.

3.3. Compression for Federated Learning

In this section, we point another compression problem that can benefit from successive pruning strategy. In federated learning, a NN model is trained across multiple edge devices, each having local training data (Konečný et al., 2016a). Each device is responsible for doing some local training over the local data and sending the local gradients to a centralized processor. The communication of gradients at each round is costly as the gradients are in model size. Given the resource

limitations of edge devices, gradient communication is a significant bottleneck in federated learning, and gradient compression is crucial (Konečný et al., 2016b).

We present density plots of gradients in Appendix D, supporting that Laplacian distribution is a good fit for NN gradients during different stages of the training, and exponential distribution almost perfectly matches the distribution of sign-free gradients. Following the same reasoning in model compression, we propose the successive pruning strategy for compressing the sign-free gradients in federated learning. Similar to the case in pruning, existing sparsification methods for local gradients do not propose an efficient encoding scheme for sparsified gradients (Lin et al., 2017b; McMahan et al., 2017; Aji & Heafield, 2017; Wang et al., 2018; Wangni et al., 2018; Barnes et al., 2020). With successive pruning, we provide a novel gradient sparsification strategy followed by Golomb coding that requires an order of magnitude less communication budget to send the compressed gradients compared to prior work.

4. Experiments

We present successive pruning results in Section 4.1, and some preliminary results on compression for federated learning in Section 4.2. We ran the experiments 3 times as our method involves random permutation and selection.

We consider three image datasets: MNIST (LeCun et al., 2010), CIFAR-10 (Krizhevsky et al., 2009) and ImageNet (Deng et al., 2009). For the MNIST experiments, we use two architectures: LeNet-5-Caffe, and LeNet-300-100 (LeCun et al., 1998). For CIFAR-10, we use two architectures: ResNet-18 (He et al., 2016) and small VGG-16 (Simonyan & Zisserman, 2014). For ImageNet, we use pretrained ResNet-50 from PyTorch (He et al., 2016; Paszke et al., 2019). We give additional details on model architectures and hyperparameters in Appendix E.

4.1. Model Compression

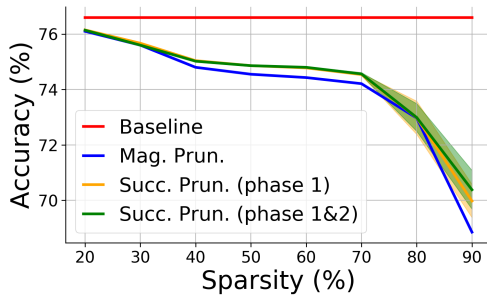
For the accuracy-sparsity trade-off, we compare our scheme with magnitude pruning (Han et al., 2016) since (Frankle et al., 2020) show that magnitude pruning performs better than many alternative pruning frameworks (Lee et al., 2018; Frankle & Carbin, 2019; Wang et al., 2020a; Tanaka et al., 2020). For both successive pruning and magnitude pruning, we retrained the pruned model for 20 epochs. Although we applied one-shot pruning, i.e., prune once and retrain once, for both methods, it is straightforward to extend successive pruning with several phase-1’s followed by one phase-2 to perform iterative pruning with increasing sparsity ratios. We show in Figure 6 that successive pruning consistently achieves better test accuracy than magnitude pruning under the same sparsity constraint on ImageNet and CIFAR-10

datasets with ResNet-50, ResNet-18, and small VGG-16. We present additional results on MNIST with LeNet-5-Caffe and LeNet-300-100 in Appendix F. The improvement of successive pruning is more evident in higher sparsity ratios. For instance, magnitude pruning with 95% sparsity results in 10% test accuracy (random prediction) for VGG-16 on CIFAR-10, whereas successive pruning achieves 90% accuracy with the same sparsity (see Figure 6(c)).

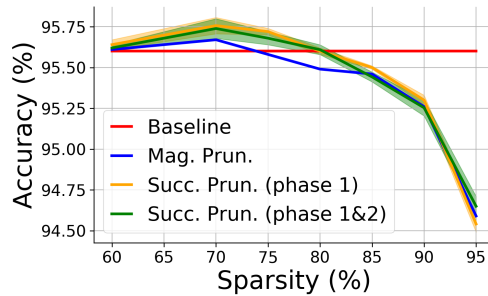
Model (Original size)	Original Acc. (%)	Method	Sparsity $\frac{ w_{\neq 0} }{ w }$ (%)	Comp. Size	Comp. Acc. (%)
LeNet-5-Caffe MNIST (1.72 MB)	99.1	Deep Comp.	92.0	44 KB ($\times 39$)	99.3
		DNS	99.1	16 KB ($\times 107$)	99.1
		SWS	99.5	11 KB ($\times 156$)	99.0
		DeepCABAC	98.1	12 KB ($\times 143$)	99.1
		Succ. Prun.(1&2)	99.2	7 KB ($\times 246$)	99.0
		Succ. Prun.(1&2)	99.3	5 KB ($\times 344$)	98.0
LeNet-300-100 MNIST (1.06 MB)	98.6	Deep Comp.	92.0	27 KB ($\times 40$)	98.4
		SWS	95.7	16.7 KB ($\times 64$)	98.1
		DeepCABAC	91.0	19.4 KB ($\times 54$)	98.0
		Succ. Prun.(1&2)	96.5	14.8 KB ($\times 72$)	98.1
		Succ. Prun.(1&2)	98.0	6.9 KB ($\times 155$)	97.1
		ResNet-50 ImageNet (102.23 MB)	76.6	Deep Comp.	71.0
DeepCABAC	74.6	6.1 MB ($\times 16$)		74.1	
Succ. Prun.(1&2)	90.0	7.5 MB ($\times 13$)		70.2	
Succ. Prun.(1&2)	70.0	17.3 MB ($\times 6$)		74.6	
Succ. Prun.(1)	71.0	6.1 MB ($\times 16$)		74.6	

Table 1. Comparison of Successive Pruning with Other Pruning Strategies in terms of Accuracy, Sparsity and Size. Succ. Prun.(1&2): Successive Pruning in both phases; Succ. Prun.(1): Successive Pruning in phase-1 + CSR and Huffman in phase-2; Deep Comp.: (Han et al., 2016); DNS: (Guo et al., 2016); SWS: (Ullrich et al., 2017); DeepCABAC: (Wiedemann et al., 2020).

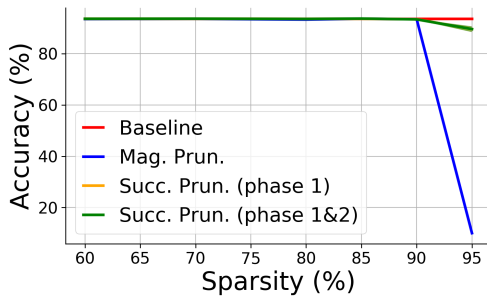
We also compare successive pruning with Deep Compression (Han et al., 2016), Dynamic Network Surgery (Guo et al., 2016), Soft Weight Sharing (Ullrich et al., 2017), and DeepCABAC (Wiedemann et al., 2020) in terms of pruned model’s size in Table 1. For conciseness, we give the average numbers over 3 runs and refer the reader to Appendix F for more detailed results (5 architectures, 3 datasets) with confidence intervals. Notice that successive pruning reduces the model size by 344 and 155 times for LeNet-5-Caffe and LeNet-300-100 while still preserving the original accuracy on MNIST. This is an improvement by 2.5 times in the compression rate compared to the previous work. However, for ResNet-50, the memory efficiency that successive pruning provides is not higher than the previous work. We believe that this is due to the different sparsity levels between MNIST and ImageNet tasks. For the moderate sparsity levels, e.g., 71% in ResNet-50, CSR representation in (Han et al., 2016) is efficient with three tricks: (1) the encoder encodes the relative index between nonzero weights instead of actual indices, (2) there exists a maximum span of relative indices, and (3) the encoder inserts a filler zero when there is no nonzero weight to be encoded in the allowed span. These tricks lead to inefficient encoding when the sparsity ratio is high, e.g., LeNet-5-Caffe with 99% sparsity, because it requires either (i) a larger span of the relative



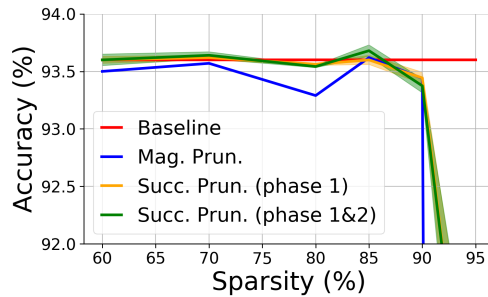
(a) ResNet-50 on ImageNet.



(b) ResNet-18 on CIFAR-10.



(c) Small VGG-16 on CIFAR-10 (10-94 % Accuracy).



(d) Small VGG-16 on CIFAR-10 (92-94 % Accuracy).

Figure 6. Comparison of Mag. Prun.: magnitude pruning (Han et al., 2016); Succ. Prun. (phase 1): successive pruning in phase-1+retraining; Succ. Prun. (phase 1&2): successive pruning in phase-1+retraining+successive pruning in phase-2. Successive pruning experiments are conducted 3 times.

indices with more bits per index, or (ii) additional redundant filler zeros. Thus, after applying successive pruning in phase-1; our procedure for phase-2 is to (a) apply successive pruning when the model sparsity is high, and (b) apply CSR representation with Huffman coding (Han et al., 2016) or DeepCABAC (Wiedemann et al., 2020) when the model sparsity is low. The last row of Table 1 shows that successive pruning in phase-1 followed by CSR representation and Huffman coding in phase-2 outperforms previous work in accuracy-size trade-off.

We consider the approaches of (Oktay et al., 2019; Havasi et al., 2019) orthogonal to our work for two reasons: (1) they modify the training process, which is different from our problem of compressing any given trained model, and (2) their reconstruction is not sparse while our primary focus is a sparse representation that provides faster computation.

4.2. Compression for Federated Learning

In our preliminary experiments on federated learning of LeNet-5-Caffe on MNIST with 10 devices, we compare successive pruning with Deep Gradient Compression (DGC) (Lin et al., 2017b) which communicates the top- k largest gradients and rTop- k (Barnes et al., 2020) which commu-

nicates randomly selected k gradients among the largest r gradients. We compute the communication budget for prior work by assuming a naive encoding with $k(\log n + 32)$ bits (n is the number of model parameters) since no efficient encoding method is provided. With the same sparsity ratio 99.9%, DGC achieves 98.5% accuracy with 2.05KB of budget, rTop- k achieves 99.1% accuracy with 2.05KB of budget, and successive pruning achieves 99.1% accuracy with 218B of budget. Thus, successive pruning provides an order of magnitude improvement in the gradients’ compression rate while achieving the same accuracy as rTop- k .

5. Conclusion

In this work, we studied NN compression problem from an information-theoretic approach and found out that rate distortion theory suggests pruning as an optimal NN compression technique. We introduced an end-to-end model compression pipeline which involves a novel pruning strategy. We suggested that our strategy is optimal for gradient compression in communication-efficient federated learning as well. Developing more efficient entropy coding methods for a “sparse exponential source” would be interesting future work.

6. Acknowledgement

This work was supported in part by a Sony Stanford Graduate Fellowship.

References

- Aji, A. F. and Heafield, K. Sparse communication for distributed gradient descent. *arXiv preprint arXiv:1704.05021*, 2017.
- Anwar, S., Hwang, K., and Sung, W. Structured pruning of deep convolutional neural networks. *ACM Journal on Emerging Technologies in Computing Systems (JETC)*, 13(3):1–18, 2017.
- Barnes, L. P., Inan, H. A., Isik, B., and Özgür, A. rtop-k: A statistical estimation approach to distributed sgd. *IEEE Journal on Selected Areas in Information Theory*, 1(3): 897–907, 2020. doi: 10.1109/JSAIT.2020.3042094.
- Berger, T. Rate-distortion theory. *Wiley Encyclopedia of Telecommunications*, 2003.
- Blalock, D., Ortiz, J. J. G., Frankle, J., and Gutttag, J. What is the state of neural network pruning? *arXiv preprint arXiv:2003.03033*, 2020.
- Bucilua, C., Caruana, R., and Niculescu-Mizil, A. Model compression. In *Proceedings of the 12th ACM SIGKDD International Conference on Knowledge Discovery and Data Mining*, KDD '06, pp. 535–541, New York, NY, USA, 2006. Association for Computing Machinery. ISBN 1595933395. doi: 10.1145/1150402.1150464. URL <https://doi.org/10.1145/1150402.1150464>.
- Carreira-Perpinán, M. A. and Idelbayev, Y. “learning-compression” algorithms for neural net pruning. In *Proceedings of the IEEE Conference on Computer Vision and Pattern Recognition*, pp. 8532–8541, 2018.
- Castellano, G., Fanelli, A. M., and Pelillo, M. An iterative pruning algorithm for feedforward neural networks. *IEEE transactions on Neural networks*, 8(3):519–531, 1997.
- Cheng, Y., Wang, D., Zhou, P., and Zhang, T. Model compression and acceleration for deep neural networks: The principles, progress, and challenges. *IEEE Signal Processing Magazine*, 35(1):126–136, 2018.
- Cover, T. M. and Thomas, J. A. *Elements of Information Theory (Wiley Series in Telecommunications and Signal Processing)*. Wiley-Interscience, USA, 2006. ISBN 0471241954.
- Cun, Y. L., Denker, J. S., and Solla, S. A. *Optimal Brain Damage*, pp. 598–605. Morgan Kaufmann Publishers Inc., San Francisco, CA, USA, 1990. ISBN 1558601007.
- Dean, J., Corrado, G., Monga, R., Chen, K., Devin, M., Mao, M., Ranzato, M., Senior, A., Tucker, P., Yang, K., et al. Large scale distributed deep networks. In *Advances in neural information processing systems*, pp. 1223–1231, 2012.
- Deng, J., Dong, W., Socher, R., Li, L.-J., Li, K., and Fei-Fei, L. ImageNet: A Large-Scale Hierarchical Image Database. In *CVPR09*, 2009.
- Engelbrecht, A. P. A new pruning heuristic based on variance analysis of sensitivity information. *IEEE transactions on Neural Networks*, 12(6):1386–1399, 2001.
- Equitz, W. H. and Cover, T. M. Successive refinement of information. *IEEE Transactions on Information Theory*, 37(2):269–275, 1991.
- Frankle, J. and Carbin, M. The lottery ticket hypothesis: Finding sparse, trainable neural networks. *International Conference on Learning Representations (ICLR)*, 2019.
- Frankle, J., Dziugaite, G. K., Roy, D. M., and Carbin, M. Pruning neural networks at initialization: Why are we missing the mark? *arXiv preprint arXiv:2009.08576*, 2020.
- Gale, T., Elsen, E., and Hooker, S. The state of sparsity in deep neural networks. *arXiv preprint arXiv:1902.09574*, 2019.
- Gallager, R. and Van Voorhis, D. Optimal source codes for geometrically distributed integer alphabets (corresp.). *IEEE Transactions on Information theory*, 21(2):228–230, 1975.
- Gao, W., Liu, Y.-H., Wang, C., and Oh, S. Rate distortion for model compression: From theory to practice. In *International Conference on Machine Learning*, pp. 2102–2111. PMLR, 2019.
- Golomb, S. Run-length encodings (corresp.). *IEEE transactions on information theory*, 12(3):399–401, 1966.
- Guo, Y., Yao, A., and Chen, Y. Dynamic network surgery for efficient dnns. In *Advances in neural information processing systems*, pp. 1379–1387, 2016.
- Han, S., Pool, J., Tran, J., and Dally, W. Learning both weights and connections for efficient neural network. In *Advances in neural information processing systems*, pp. 1135–1143, 2015.
- Han, S., Mao, H., and Dally, W. J. Deep compression: Compressing deep neural networks with pruning, trained quantization and huffman coding. *International Conference on Learning Representations (ICLR)*, 2016.

- Hassibi, B., Stork, D. G., Wolff, G., and Watanabe, T. Optimal brain surgeon: Extensions and performance comparisons. In *Proceedings of the 6th International Conference on Neural Information Processing Systems, NIPS'93*, pp. 263–270, San Francisco, CA, USA, 1993.
- Havasi, M., Peharz, R., and Hernández-Lobato, J. M. Minimal random code learning: Getting bits back from compressed model parameters. In *International Conference on Learning Representations (ICLR)*, 2019.
- He, K., Zhang, X., Ren, S., and Sun, J. Deep residual learning for image recognition. In *Proceedings of the IEEE conference on computer vision and pattern recognition*, pp. 770–778, 2016.
- He, Y., Zhang, X., and Sun, J. Channel pruning for accelerating very deep neural networks. In *Proceedings of the IEEE International Conference on Computer Vision*, pp. 1389–1397, 2017.
- Huffman, D. A. A method for the construction of minimum-redundancy codes. *Proceedings of the IRE*, 40(9):1098–1101, 1952.
- Isik, B., Choi, K., Zheng, X., Weissman, T., Ermon, S., Wong, H. S. P., and Alaghi, A. Neural network compression for noisy storage devices. *arXiv preprint arXiv:2102.07725*, 2021.
- Kairouz, P., McMahan, H. B., Avent, B., Bellet, A., Bennis, M., Bhagoji, A. N., Bonawitz, K., Charles, Z., Cormode, G., Cummings, R., et al. Advances and open problems in federated learning. *arXiv preprint arXiv:1912.04977*, 2019.
- Konečný, J., McMahan, H. B., Ramage, D., and Richtárik, P. Federated optimization: Distributed machine learning for on-device intelligence. *CoRR*, abs/1610.02527, 2016a.
- Konečný, J., McMahan, H. B., Yu, F. X., Richtárik, P., Suresh, A. T., and Bacon, D. Federated learning: Strategies for improving communication efficiency. In *NIPS Workshop on Private Multi-Party Machine Learning*, 2016b.
- Koshelev, V. N. Hierarchical coding of discrete sources. *Problemy peredachi informatsii*, 16(3):31–49, 1980.
- Krizhevsky, A., Hinton, G., et al. Learning multiple layers of features from tiny images. 2009.
- LeCun, Y., Bottou, L., Bengio, Y., and Haffner, P. Gradient-based learning applied to document recognition. *Proceedings of the IEEE*, 86(11):2278–2324, 1998.
- LeCun, Y., Cortes, C., and Burges, C. Mnist handwritten digit database, 2010.
- LeCun, Y., Bengio, Y., and Hinton, G. Deep learning. *nature*, 521(7553):436–444, 2015.
- Lee, N., Ajanthan, T., and Torr, P. H. Snip: Single-shot network pruning based on connection sensitivity. *arXiv preprint arXiv:1810.02340*, 2018.
- Lin, J., Rao, Y., Lu, J., and Zhou, J. Runtime neural pruning. In *Proceedings of the 31st International Conference on Neural Information Processing Systems*, pp. 2178–2188, 2017a.
- Lin, S., Ji, R., Yan, C., Zhang, B., Cao, L., Ye, Q., Huang, F., and Doermann, D. Towards optimal structured cnn pruning via generative adversarial learning. In *Proceedings of the IEEE/CVF Conference on Computer Vision and Pattern Recognition*, pp. 2790–2799, 2019.
- Lin, Y., Han, S., Mao, H., Wang, Y., and Dally, W. J. Deep gradient compression: Reducing the communication bandwidth for distributed training. *International Conference on Learning Representations (ICLR)*, 2017b.
- Liu, Z., Sun, M., Zhou, T., Huang, G., and Darrell, T. Rethinking the value of network pruning. *arXiv preprint arXiv:1810.05270*, 2018a.
- Liu, Z., Xu, J., Peng, X., and Xiong, R. Frequency-domain dynamic pruning for convolutional neural networks. In *Proceedings of the 32nd International Conference on Neural Information Processing Systems*, pp. 1051–1061, 2018b.
- Liu, Z., Mu, H., Zhang, X., Guo, Z., Yang, X., Cheng, K.-T., and Sun, J. Metapruning: Meta learning for automatic neural network channel pruning. In *Proceedings of the IEEE/CVF International Conference on Computer Vision*, pp. 3296–3305, 2019.
- Marpe, D. and Wiegand, T. A highly efficient multiplication-free binary arithmetic coder and its application in video coding. In *Proceedings 2003 International Conference on Image Processing (Cat. No. 03CH37429)*, volume 2, pp. II–263. IEEE, 2003.
- McMahan, H. B., Moore, E., Ramage, D., Hampson, S., and y Arcas, B. A. Communication-efficient learning of deep networks from decentralized data. In *AISTATS*, 2017.
- Molchanov, D., Ashukha, A., and Vetrov, D. Variational dropout sparsifies deep neural networks. In *International Conference on Machine Learning*, pp. 2498–2507. PMLR, 2017.
- Molchanov, P., Tyree, S., Karras, T., Aila, T., and Kautz, J. Pruning convolutional neural networks for resource efficient inference. *arXiv preprint arXiv:1611.06440*, 2016.

- No, A. and Weissman, T. Rateless lossy compression via the extremes. *IEEE transactions on information theory*, 62(10):5484–5495, 2016.
- Oktay, D., Ballé, J., Singh, S., and Shrivastava, A. Scalable model compression by entropy penalized reparameterization. In *International Conference on Learning Representations (ICLR)*, 2019.
- Paszke, A., Gross, S., Massa, F., Lerer, A., Bradbury, J., Chanan, G., Killeen, T., Lin, Z., Gimelshein, N., Antiga, L., Desmaison, A., Kopf, A., Yang, E., DeVito, Z., Raison, M., Tejani, A., Chilamkurthy, S., Steiner, B., Fang, L., Bai, J., and Chintala, S. Pytorch: An imperative style, high-performance deep learning library. In Wallach, H., Larochelle, H., Beygelzimer, A., d'Alché-Buc, F., Fox, E., and Garnett, R. (eds.), *Advances in Neural Information Processing Systems 32*, pp. 8024–8035. Curran Associates, Inc., 2019.
- Peng, H., Wu, J., Chen, S., and Huang, J. Collaborative channel pruning for deep networks. In *International Conference on Machine Learning*, pp. 5113–5122. PMLR, 2019.
- Sehwag, V., Wang, S., Mittal, P., and Jana, S. Hydra: Pruning adversarially robust neural networks. *Advances in Neural Information Processing Systems (NeurIPS)*, 7, 2020.
- Shannon, C. E. A mathematical theory of communication. *ACM SIGMOBILE mobile computing and communications review*, 5(1):3–55, 2001.
- Simonyan, K. and Zisserman, A. Very deep convolutional networks for large-scale image recognition. *arXiv preprint arXiv:1409.1556*, 2014.
- Singh, S. P. and Alistarh, D. Woodfisher: Efficient second-order approximations for model compression. *arXiv preprint arXiv:2004.14340*, 2020.
- Srinivas, S. and Babu, R. V. Data-free parameter pruning for deep neural networks. *arXiv preprint arXiv:1507.06149*, 2015.
- Tanaka, H., Kunin, D., Yamins, D. L., and Ganguli, S. Pruning neural networks without any data by iteratively conserving synaptic flow. *arXiv preprint arXiv:2006.05467*, 2020.
- Ullrich, K., Meeds, E., and Welling, M. Soft weight-sharing for neural network compression. *arXiv preprint arXiv:1702.04008*, 2017.
- Van Leeuwen, J. On the construction of huffman trees. In *ICALP*, pp. 382–410, 1976.
- Venkataramanan, R., Sarkar, T., and Tatikonda, S. Lossy compression via sparse linear regression: Computationally efficient encoding and decoding. *IEEE transactions on information theory*, 60(6):3265–3278, 2014.
- Verdu, S. The exponential distribution in information theory. *Problemy peredachi informatsii*, 32(1):100–111, 1996.
- Wang, C., Zhang, G., and Grosse, R. Picking winning tickets before training by preserving gradient flow. *arXiv preprint arXiv:2002.07376*, 2020a.
- Wang, H., Sievert, S., Liu, S., Charles, Z. B., Papailiopoulos, D. S., and Wright, S. Atomo: Communication-efficient learning via atomic sparsification. In *NeurIPS*, 2018.
- Wang, Y., Zhang, X., Xie, L., Zhou, J., Su, H., Zhang, B., and Hu, X. Pruning from scratch. In *Proceedings of the AAAI Conference on Artificial Intelligence*, volume 34, pp. 12273–12280, 2020b.
- Wangni, J., Wang, J., Liu, J., and Zhang, T. Gradient sparsification for communication-efficient distributed optimization. In Bengio, S., Wallach, H., Larochelle, H., Grauman, K., Cesa-Bianchi, N., and Garnett, R. (eds.), *Advances in Neural Information Processing Systems 31*, pp. 1299–1309. Curran Associates, Inc., 2018.
- Wiedemann, S., Kirchhoffer, H., Matlage, S., Haase, P., Marban, A., Marinč, T., Neumann, D., Nguyen, T., Schwarz, H., Wiegand, T., Marpe, D., and Samek, W. Deepcabac: A universal compression algorithm for deep neural networks. *IEEE Journal of Selected Topics in Signal Processing*, 14(4):700–714, 2020.
- Williams, P. M. Bayesian regularization and pruning using a laplace prior. *Neural computation*, 7(1):117–143, 1995.
- Xiao, X., Wang, Z., and Rajasekaran, S. Autoprune: Automatic network pruning by regularizing auxiliary parameters. *Advances in neural information processing systems*, 32, 2019.
- Yang, T.-J., Chen, Y.-H., and Sze, V. Designing energy-efficient convolutional neural networks using energy-aware pruning. In *Proceedings of the IEEE Conference on Computer Vision and Pattern Recognition (CVPR)*, July 2017.
- Yu, R., Li, A., Chen, C.-F., Lai, J.-H., Morariu, V. I., Han, X., Gao, M., Lin, C.-Y., and Davis, L. S. Nisp: Pruning networks using neuron importance score propagation. In *Proceedings of the IEEE Conference on Computer Vision and Pattern Recognition*, pp. 9194–9203, 2018.
- Zhao, C., Ni, B., Zhang, J., Zhao, Q., Zhang, W., and Tian, Q. Variational convolutional neural network pruning. In *Proceedings of the IEEE/CVF Conference on Computer Vision and Pattern Recognition*, pp. 2780–2789, 2019.

Appendix

A. Density Estimation of Neural Network Parameters

In Section 2.1, we have justified our assumption of exponential distribution over sign-free NN weights by demonstrating the density of ResNet-18 weights trained on CIFAR-10. To further support our argument, we present density plots of other architectures trained on different datasets in Figure 7. We show that exponential distribution is a good fit for sign-free weights of ResNet-50 trained on ImageNet, small VGG-16 trained on CIFAR-10, and LeNet-5-Caffe trained on MNIST. We have also examined the weight distribution layer by layer. We have observed that weights of layers closer to the input tend to follow a Gaussian-like distribution. In contrast, the weights of layers closer to the output behave like Laplacian random variables. Since the last layers are more parameterized in the architectures used in this work, we see a Laplacian distribution over the weights globally. Different pruning strategies might be necessary for layers with Gaussian and Laplacian behaviour for a layer by layer pruning approach.

B. Compression for Exponential Source

B.1. LOSSY COMPRESSION

In this section, we briefly describe the proof outline of Lemma 1 as well as Eq. 4 which is provided in (Verdu, 1996).

Proof of Lemma 1. Consider the exponential source $\mathbf{U} \sim P_{\mathbf{U}}$ with parameter λ , and the target distortion D satisfies $0 \leq D \leq 1/\lambda$. Then,

$$\begin{aligned} R(D) &= \min_{\mathbb{E}[d(\mathbf{U}, \hat{\mathbf{U}})] \leq D} I(\mathbf{U}; \hat{\mathbf{U}}) \\ &= \inf_{\mathbb{E}[\mathbf{U} - \hat{\mathbf{U}}] \leq D, \hat{\mathbf{U}} \leq \mathbf{U}} I(\mathbf{U}; \hat{\mathbf{U}}). \end{aligned}$$

Let Q be another conditional distribution where $Q_{\mathbf{U}|\hat{\mathbf{U}}}(u|\hat{u}) = \frac{1}{D} e^{-(u-\hat{u})/D}$. Then,

$$\begin{aligned} I(\mathbf{U}; \hat{\mathbf{U}}) &= D_{KL}(P_{\mathbf{U}|\hat{\mathbf{U}}} \| P_{\mathbf{U}} | \hat{\mathbf{U}}) \\ &= D_{KL}(P_{\mathbf{U}|\hat{\mathbf{U}}} \| Q_{\mathbf{U}|\hat{\mathbf{U}}} | P_{\hat{\mathbf{U}}}) \\ &\quad + \mathbb{E}_{P_{\mathbf{U}, \hat{\mathbf{U}}}} \left[\log \frac{Q_{\mathbf{U}|\hat{\mathbf{U}}}(\mathbf{U}|\hat{\mathbf{U}})}{P_{\mathbf{U}}(\mathbf{U})} \right] \\ &\geq \mathbb{E}_{P_{\mathbf{U}, \hat{\mathbf{U}}}} \left[\log \frac{Q_{\mathbf{U}|\hat{\mathbf{U}}}(\mathbf{U}|\hat{\mathbf{U}})}{P_{\mathbf{U}}(\mathbf{U})} \right] \end{aligned} \quad (5)$$

$$\begin{aligned} &= -\log(\lambda D) + 1 - \frac{1}{\lambda D} + \frac{1}{D} \mathbb{E}[\hat{\mathbf{U}}] \\ &\geq -\log(\lambda D). \end{aligned} \quad (6)$$

This implies that $R(D) \geq -\log(\lambda D)$.

On the other hand, let \mathbf{V} be a mixture of point measure and exponential random variable, where the probability density function is given by

$$P_{\mathbf{V}}(v) = \lambda D \cdot \delta(v) + (1 - \lambda D) \cdot \lambda e^{-\lambda v}.$$

We further let \mathbf{N} be an exponential random variable with parameter $1/D$, where \mathbf{V} and \mathbf{N} are independent. Then, the Laplace transform of $P_{\mathbf{V}}$ and $P_{\mathbf{N}}$ are given by

$$\begin{aligned} \mathbb{E}[e^{-s\mathbf{V}}] &= \lambda D + (1 - \lambda D) \frac{\lambda}{\lambda + s} \\ \mathbb{E}[e^{-s\mathbf{N}}] &= \frac{1/D}{1/D + s}. \end{aligned}$$

Then,

$$\begin{aligned} \mathbb{E}[e^{-s(\mathbf{V}+\mathbf{N})}] &= \mathbb{E}[e^{-s\mathbf{V}}] \cdot \mathbb{E}[e^{-s\mathbf{N}}] \\ &= \frac{\lambda}{\lambda + s}, \end{aligned}$$

which is the Laplace transform of $P_{\mathbf{U}}$. In other words, $\mathbf{U} \stackrel{(d)}{=} \mathbf{V} + \mathbf{N}$. Thus, by letting $\mathbf{U} = \mathbf{V} + \mathbf{N}$, we obtain the conditional distribution $Q_{\mathbf{U}|\mathbf{V}}(u|v) = \frac{1}{D} e^{-(u-v)/D}$. It is clear that $Q_{\mathbf{U}|\mathbf{V}}$ satisfies the equality conditions in Eq. 5 and Eq. 6, and therefore it achieves the lower bound $I(\mathbf{U}; \mathbf{V}) = -\log(\lambda D)$ with $\hat{\mathbf{U}} = \mathbf{V}$.

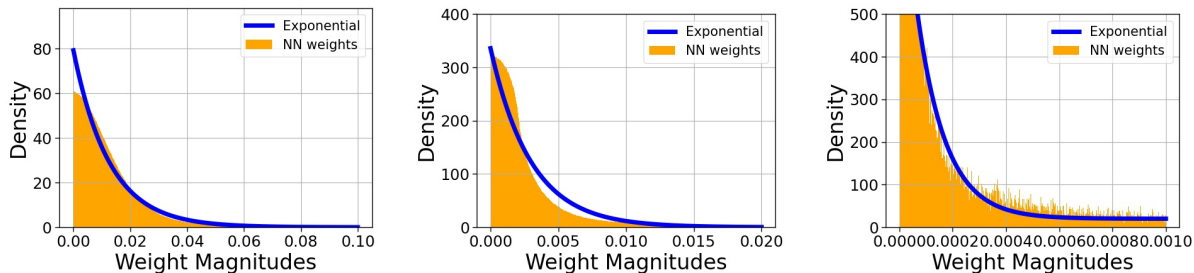
To sum, the optimal rate distortion trade-off is $R(D) = -\log(\lambda D)$ and it can be achieved with a reconstruction that follows

$$P_{\mathbf{V}}(v) = \lambda D \cdot \delta(v) + (1 - \lambda D) \cdot \lambda e^{-\lambda v}. \quad (7)$$

□

Lemma 1 and Eq. 4 indicate that:

- (1) The optimal encoder-decoder pair, i.e., compression scheme, makes the reconstruction sparse as Eq. 4 is a sparse exponential distribution where λD fraction of the elements are 0. More concretely, the reconstructed NN model decoded from the compressed representation must be sparse to satisfy the conditions for the optimal compression scheme. In other words, rate distortion theory suggests pruning for NN compression.
- (2) Once \mathbf{V} is reconstructed on the decoder side, the error term on the encoder side, $\mathbf{U} - \mathbf{V}$, follows an exponential distribution with parameter $1/D$. This property allows for a successively refinable coding scheme with low complexity. Namely, we can iteratively describe NN weights with a reasonable complexity at each iteration.



(a) Density of ResNet-50 Sign-Free Weights. (b) Density of Small VGG-16 Sign-Free Weights. (c) Density of LeNet-5 Caffe Sign-Free Weights.

Figure 7. Sign-Free Weight Density of (a) ResNet-50 trained on ImageNet, (b) VGG-16 trained on CIFAR-10, (c) LeNet-5 Caffe trained on MNIST.

B.2. LOSSLESS COMPRESSION (ENTROPY CODING)

In this section, we briefly mention two entropy coding methods, unary coding and Golomb coding, that describe geometric sources efficiently.

Unary Coding. Unary coding is a prefix-free code that is optimally efficient for the following geometric distribution:

$$P_B(b) = 2^{-b} \quad (8)$$

where b is a positive integer. In the simplest term, unary coding encodes an integer b with single 1 followed by $b - 1$ consecutive 0's. For instance, 72 would be uniquely encoded as 100000010. In our problem, indices follow the distribution in Eq. 8 only when the fraction of sign-free weights larger than $1/\lambda_t$ is exactly equal to $1/2$. Since this is not the case in every iteration, unary coding is not the optimal entropy coding method for indices in the successive pruning algorithm.

Golomb Coding. Golomb coding is an optimal prefix-free code for any geometric source, i.e., it is more general than unary coding. Recall that in successive pruning algorithm with the random permutation trick described in Section 3.1.2, small indices are more likely to be selected than the large ones. This makes Golomb coding a promising entropy coding method for successive pruning. The construction of Golomb codes can be found in (Golomb, 1966).

In our experiments, we implemented Golomb coding to represent NN models as binary arrays.

C. Successive Pruning

The 2-phase successive pruning algorithm is illustrated in Figures 8, 9, and 10 with VGG-16 trained on CIFAR-10. We show the average distortion, sparsity, and accuracy of the reconstructed model through iterations of successive

pruning algorithm in Figure 8 when successive pruning is applied once without retraining. When successive pruning is applied in 2 phases, we set a desired (target) sparsity level. In Figures 9 and 10, desired sparsity is set to 90%. As can be seen from Figure 9(b), phase-1 of successive pruning stops when the sparsity is equal to 90%. Notice from Figure 9(c) that the accuracy of the reconstructed model is only 10% (random prediction) when phase-1 ends. After this reconstructed model (output of phase-1) is retrained for 20 epochs, phase-2 starts. We show the change in the distortion, sparsity, and accuracy on the reconstructed model during phase-2 in Figure 10. It is seen from Figure 10(b) that sparsity does not change once it drops to the desired sparsity 90%, while accuracy increases up to the baseline accuracy in Figure 10(c).

Lastly, we show the density of nonzero sign-free weights after phase-1 and retraining in Figure 11. Since exponential distribution is still a good fit, we can apply successive pruning in phase-2.

D. Compression for Federated Learning

In Section 3.3, we have proposed successive pruning to compress gradients in federated learning. In Figures 12, 13, and 14, we justify that Laplacian and exponential distributions are good fits for gradients and sign-free gradients of ResNet-50 trained on ImageNet, ResNet-18 trained on CIFAR-10 and VGG-16 trained on CIFAR-10. Since we need to compress the gradients before each communication round of federated training, successive pruning requires the sign-free gradients to follow an exponential distribution throughout the learning process. In other words, although the parameter of the exponential distribution might change, we must be able to fit an exponential distribution to the sign-free gradients in every round. We provide the density estimation of sign-free gradients in early-, mid-, and late-stages of training in Figures 12, 13, and 14 to show that exponential

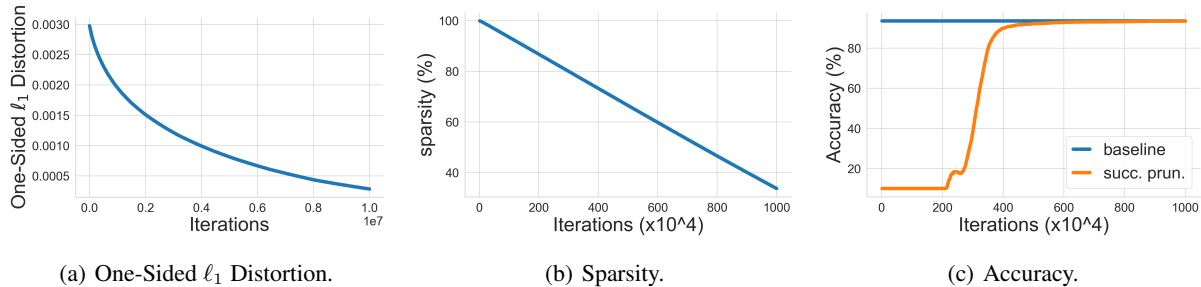


Figure 8. (a) Average one-sided ℓ_1 distortion, (b) sparsity, (c) accuracy of the reconstructed VGG-16 when successive pruning is applied without retraining (only phase-1). Baseline: fully-trained model without compression, succ. prun.: successive pruning.

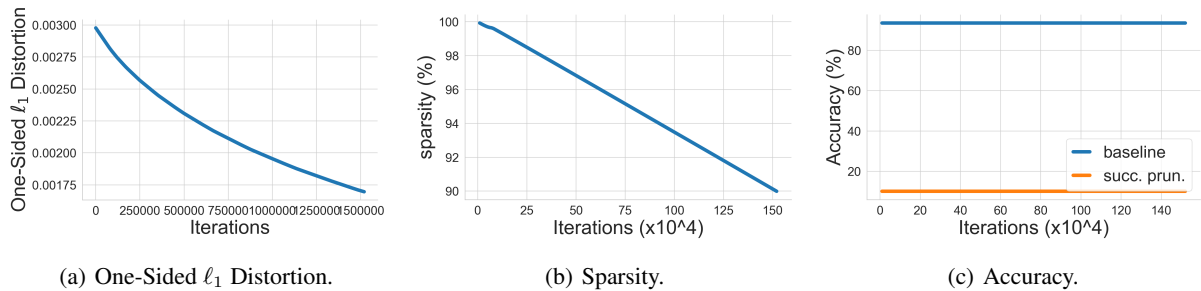


Figure 9. (a) Average one-sided ℓ_1 distortion, (b) sparsity, (c) accuracy of the reconstructed VGG-16 during phase-1 of successive pruning (before retraining). Phase-1 stops at the desired sparsity 90%. Baseline: fully-trained model without compression, succ. prun.: successive pruning.

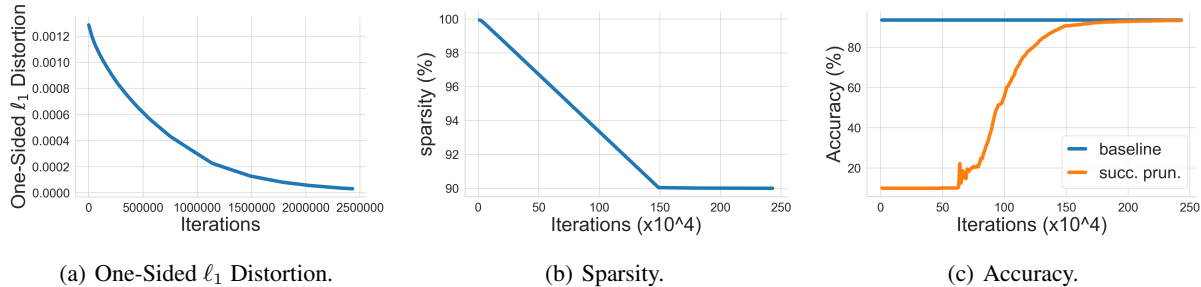


Figure 10. (a) Average one-sided ℓ_1 distortion, (b) sparsity, (c) accuracy of the reconstructed VGG-16 during phase-2 of successive pruning (after retraining). The desired sparsity is set as 90%. Baseline: fully-trained model without compression, succ. prun.: successive pruning.

distribution is a good fit for sign-free gradients starting from the early stages of training till the training ends. Therefore, we can apply successive pruning to compress gradients at every communication round. In our experiments, we update the parameter of the exponential distribution (λ) at every communication round.

Among other gradient sparsification methods for federated learning, successive pruning is most similar to rTop- k (Barnes et al., 2020), in that they also communicate a random subset of the large gradients. Different from our work, they approach the communication-efficient federated learn-

ing problem from a distributed statistical estimation point of view. By modeling the gradients with a sparse Bernoulli distribution, they show that the optimal compression strategy for each user (device) is to communicate a random k/r fraction of the r largest gradients. In contrast, we study the gradient compression problem from an information-theoretic approach and assume Laplacian distribution over the gradients (exponential for the sign-free gradients). With this assumption, we conclude that each user must communicate the mean of the gradients and a list of indices that are randomly selected among the gradients larger than $1/\lambda_t$ at

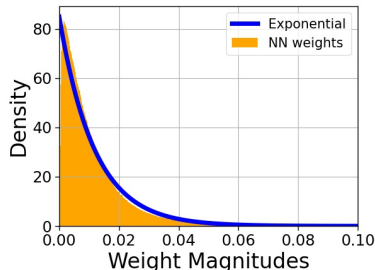


Figure 11. Density of nonzero sign-free weights of ResNet-50 trained on ImageNet after phase-1 of successive pruning and re-training. Desired (target) sparsity is 60%. Since exponential distribution is still a good fit for sign-free weights, successive pruning is applicable in phase-2.

iteration t . Since the threshold $1/\lambda_t$ is decreasing at each iteration, successive pruning assigns a higher probability for larger gradients to be selected, whereas rTop- k picks the gradients uniformly random from the large gradients.

E. Datasets, Models and Hyperparameters

E.1. MNIST:

We provide the architectural details and hyperparameters for LeNet-5 Caffe and LeNet-300-100 in Tables 2 and 3 respectively (LeCun et al., 1998). For both LeNet-5 Caffe and LeNet-300-100, we use a batch size of 100 and train for 100 epochs, early stopping at the best accuracy on validation set. We use the Adam optimizer with learning rate = 0.001, and $\beta_1 = 0.9, \beta_2 = 0.999$ with weight decay = $5e^{-4}$.

Name	Component
conv1	$[5 \times 5$ conv, 20 filters, stride 1], ReLU, 2×2 max pool
conv2	$[5 \times 5$ conv, 50 filters, stride 1], ReLU, 2×2 max pool
Linear	Linear 800 \rightarrow 500, ReLU
Output Layer	Linear 500 \rightarrow 10

Table 2. LeNet-5 Caffe convolutional architecture.

Name	Component
Linear	Linear 784 \rightarrow 300, ReLU
Linear	Linear 300 \rightarrow 100, ReLU
Output Layer	Linear 100 \rightarrow 10

Table 3. LeNet-300-100 architecture.

E.2. CIFAR-10:

We provide the architectural details and hyperparameters for the ResNet-18 (He et al., 2016) and small VGG-16 (Simonyan & Zisserman, 2014) in Tables 4 and 5, respectively. For both ResNet-18 and small VGG-16, we use a batch size of 128, we train ResNet-18 for 350 epochs and VGG-16 for 200 epochs, early stopping at the best accuracy on valida-

tion set. We use SGD with learning rate = 0.1, momentum = 0.9, and weight decay = $5e^{-4}$.

Name	Component
conv1	3×3 conv, 64 filters, stride 1, BatchNorm
Residual Block 1	3×3 conv, 64 filters $\times 2$ 3×3 conv, 64 filters
Residual Block 2	3×3 conv, 128 filters $\times 2$ 3×3 conv, 128 filters
Residual Block 3	3×3 conv, 256 filters $\times 2$ 3×3 conv, 256 filters
Residual Block 4	3×3 conv, 512 filters $\times 2$ 3×3 conv, 512 filters
Output Layer	4×4 average pool stride 1, fully-connected, softmax

Table 4. ResNet-18 architecture.

Name	Component
conv1-2	$[3 \times 3$ conv, 64 filters, stride 1, BatchNorm, ReLU] $\times 2$
max pool	2×2 , stride 2
conv3-4	$[3 \times 3$ conv, 128 filters, stride 1, BatchNorm, ReLU] $\times 2$
max pool	2×2 , stride 2
conv5-7	$[3 \times 3$ conv, 256 filters, stride 1, BatchNorm, ReLU] $\times 3$
max pool	2×2 , stride 2
conv8-10	$[3 \times 3$ conv, 512 filters, stride 1, BatchNorm, ReLU] $\times 3$
max pool	2×2 , stride 2
conv11-13	$[3 \times 3$ conv, 512 filters, stride 1, BatchNorm, ReLU] $\times 3$
max pool	2×2 , stride 2
Output Layer	1×1 average pool stride 1, fully-connected, softmax

Table 5. VGG-16 architecture.

E.3. IMAGENET:

We provide the architectural details and hyperparameters for the ResNet-50 used in our experiments in Table 6. We use the pretrained ResNet-50 from PyTorch (<https://github.com/pytorch/vision/blob/master/torchvision/models/resnet.py>), with a batch size of 64. At the end of the first phase of the successive pruning and after the magnitude pruning, we retrain the model for 5 epochs. We use SGD with learning rate = 0.001, momentum = 0.9 and weight decay = $5e^{-4}$.

Name	Component
conv1	3×3 conv, 64 filters, stride 1, BatchNorm
Residual Block 1	1×1 conv, 64 filters $\times 3$ 3×3 conv, 64 filters 1×1 conv, 256 filters
Residual Block 2	1×1 conv, 128 filters $\times 4$ 3×3 conv, 128 filters 1×1 conv, 512 filters
Residual Block 3	1×1 conv, 256 filters $\times 6$ 3×3 conv, 256 filters 1×1 conv, 1024 filters
Residual Block 4	1×1 conv, 512 filters $\times 3$ 3×3 conv, 512 filters 1×1 conv, 2048 filters
Output Layer	4×4 average pool stride 1, fully-connected, softmax

Table 6. ResNet-50 architecture.

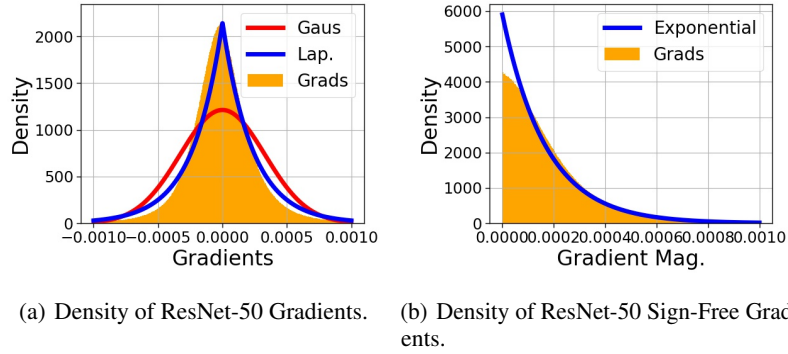


Figure 12. Density of (a) gradients of ResNet-50 trained on ImageNet, (b) sign-free gradients of ResNet-50 trained on ImageNet. We present only the gradients from the late stages of training since we use a pretrained ResNet-50.

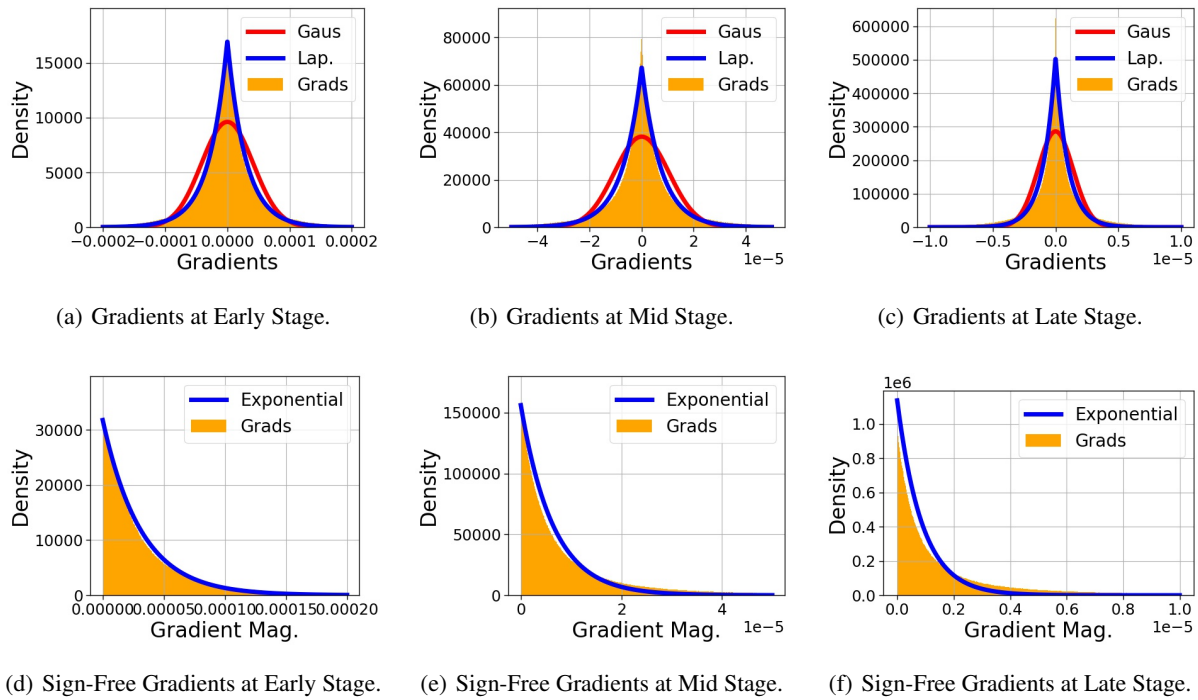


Figure 13. Density gradients of ResNet-18 trained on CIFAR-10 during (a) early stages of training (epoch 32), (b) middle stages of training (epoch 155), (c) late stages of training (epoch 336). Density of sign-free gradients of ResNet-18 trained on CIFAR-10 during (d) early stages of training (epoch 32), (e) middle stages of training (epoch 155), (f) late stages of training (epoch 336)

F. Additional Experimental Results

We give a more detailed version of Table 1 in Table 7 with confidence intervals included in successive pruning results.

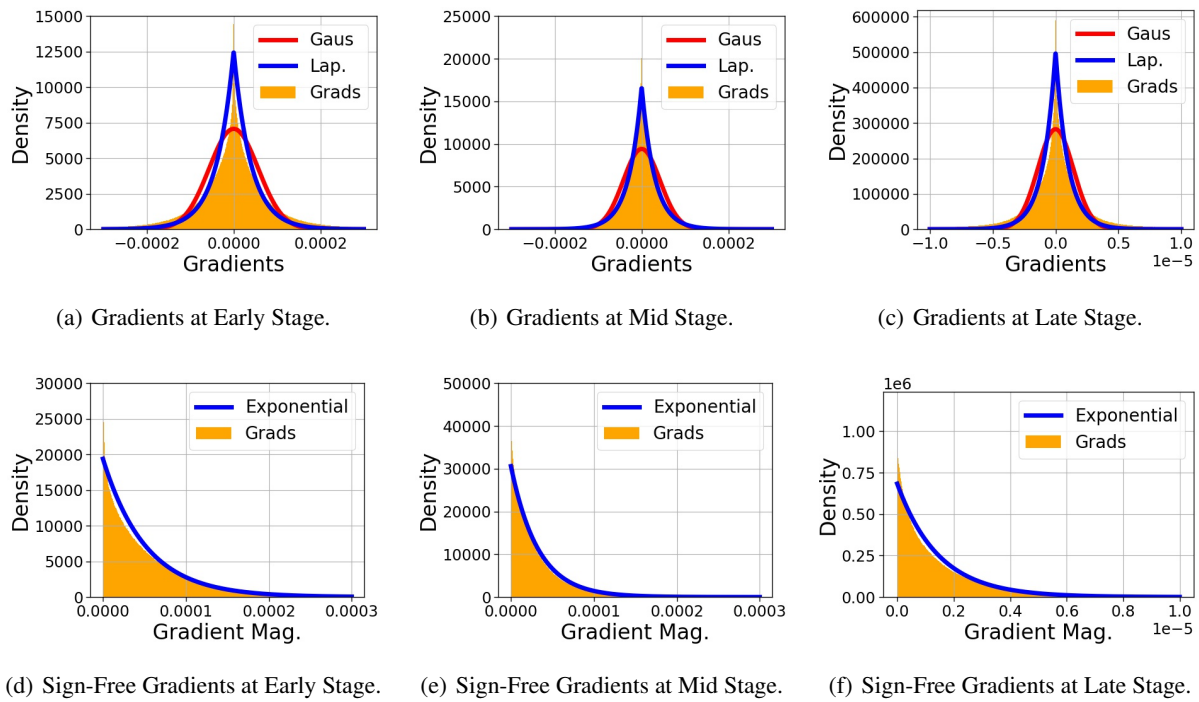


Figure 14. Density gradients of small VGG-16 trained on CIFAR-10 during (a) early stages of training (epoch 16), (b) middle stages of training (epoch 100), (c) late stages of training (epoch 170). Density of sign-free gradients of small VGG-16 trained on CIFAR-10 during (d) early stages of training (epoch 16), (e) middle stages of training (epoch 100), (f) late stages of training (epoch 170)

Model (Original size)	Original Acc. (%)	Method	Sparsity $\frac{ w=0 }{ w }$ (%)	Comp. Size	Comp. Acc. (%)
LeNet-5-Caffe MNIST (1.72 MB)	99.14	Deep Comp.	92.0	44 KB ($\times 39$)	99.3
		DNS	99.1	16 KB ($\times 107$)	99.1
		SWS	99.5	11 KB ($\times 156$)	99.0
		DeepCABAC	98.1	12 KB ($\times 143$)	99.1
		Succ. Prun.(1&2)	99.2	7 KB ($\times 246$)	99.0 (± 0.0)
		Succ. Prun.(1&2)	99.3	5 KB ($\times 344$)	98.0 (± 0.1)
LeNet-300-100 MNIST (1.06 MB)	98.6	Deep Comp.	92.0	27 KB ($\times 40$)	98.4
		SWS	95.7	16.7 KB ($\times 64$)	98.1
		DeepCABAC	91.0	19.4 KB ($\times 54$)	98.0
		Succ. Prun.(1&2)	96.5	14.8 KB ($\times 72$)	98.1 (± 0.0)
		Succ. Prun.(1&2)	98.0	6.9 KB ($\times 155$)	97.1 (± 0.1)
ResNet-18 CIFAR-10 (44.70 MB)	95.60	Succ. Prun.(1&2)	90.0	3.1 MB ($\times 15$)	95.1 (± 0.0)
		Succ. Prun.(1&2)	95.0	1.1 MB ($\times 42$)	92.2 (± 0.2)
		Succ. Prun.(1&2)	97.0	875 KB ($\times 53$)	90.0 (± 0.2)
Small VGG-16 CIFAR-10 (58.91 MB)	93.60	DeepCABAC	92.4	956 KB ($\times 61$)	91.0
		Succ. Prun.(1&2)	95.0	1.1 MB ($\times 54$)	91.1 (± 0.2)
		Succ. Prun.(1&2)	90.0	3.0 MB ($\times 20$)	93.0 (± 0.1)
ResNet-50 ImageNet (102.23 MB)	76.60	Deep Comp.	71.0	6.1 MB ($\times 16$)	76.1
		DeepCABAC	74.6	6.1 MB ($\times 16$)	74.1
		Succ. Prun.(1&2)	90.0	7.5 MB ($\times 13$)	70.2 (± 0.2)
		Succ. Prun.(1&2)	70.0	17.3 MB ($\times 6$)	74.6 (± 0.0)
		Succ.Prun.(1)	71.0	6.1 MB ($\times 16$)	74.6 (± 0.0)

Table 7. Comparison of Successive Pruning with Other Pruning Strategies in terms of Accuracy, Sparsity and Size. Succ. Prun.(1&2): Successive Pruning in both phases; Succ. Prun.(1): Successive Pruning in phase-1 + CSR and Huffman in phase-2; Deep Comp.: (Han et al., 2016); DNS: (Guo et al., 2016); SWS: (Ullrich et al., 2017); DeepCABAC: (Wiedemann et al., 2020).